Published in final edited form as:
*Anesthesiology*. 2012 October ; 117(4): 857–867. doi:10.1097/ALN.0b013e31826a8a13.

# QUANTITATIVE CHANGES IN REGIONAL CEREBRAL BLOOD FLOW INDUCED BY COLD, HEAT AND ISCHEMIC PAIN: A CONTINUOUS ARTERIAL SPIN LABELING STUDY

**Michael A. Frölich, M.D., M.S. [Associate Professor]**,
Department of Anesthesiology, University of Alabama at Birmingham, Birmingham, Alabama

**Hrishikesh Deshpande, M.S. [Programmer/Analyst]**,
Department of Psychology, University of Alabama at Birmingham, Birmingham, Alabama

**Timothy Ness, M.D, Ph.D. [Professor]**, and
Department of Anesthesiology, University of Alabama at Birmingham, Birmingham, Alabama

**Georg Deutsch, Ph.D. [Associate Professor]**
Department of Radiology, University of Alabama at Birmingham, Birmingham, Alabama

## Abstract

**Background—**The development of arterial spin labeling methods, has allowed measuring regional cerebral blood flow (rCBF) quantitatively and to show the pattern of cerebral activity associated with any state such as a sustained pain state or changes due to a neurotropic drug.

**Methods—**We studied the differential effects of three pain conditions in ten healthy subjects on a 3T scanner during resting baseline, heat, cold and ischemic pain using continuous arterial spin labeling.

**Results—**Cold pain showed the greatest absolute rCBF increases in left anterior cingulate cortex, left amygdala, left angular gyrus, and Brodmann Area 6, and a significant rCBF decrease in the cerebellum. Changes in rCBF were characteristic of the type of pain condition: cold and heat pain showed increases, while the ischemic condition showed a reduction in mean absolute gray matter flow compared to rest. An association of subjects' pain tolerance and cerebral blood flow was noted.

**Conclusions—**The observation that quantitative rCBF changes are characteristic of the pain task employed and that there is a consistent rCBF change in Brodman area 6, an area responsible for the integration of a motor response to pain, should provide extremely useful information in the quest to develop an imaging biomarker of pain. Conceivably, response in BA6 may serve as an objective measure of analgesic efficacy.

## INTRODUCTION

In recent years magnetic resonance imaging (MRI) based brain mapping techniques have significantly enhanced the ability of neuroscientists to associate brain anatomy with

Contact information: Michael A. Frölich, M.D., M.S., F619 South 19th Street, Birmigham, Alabama 35249-6810, Phone: 205-975-0145, Fax: 205-975-5963, froelich@uab.edu.



Abstract Presentation: Joint Annual Meeting ISMRM-ESMRMB 2010, April 30 to May 7, 2010, Stockholm, Sweden.

function. The vast majority of functional imaging work is based on the blood oxygen level dependent (BOLD) susceptibility difference of oxyhemoglobin and deoxyhemoglobin [1, 2] which essentially reflects capillary vasodilatation in response to regional neuronal activity in the brain. Blood oxygen dependent level functional magnetic resonance imaging (BOLD fMRI) depends on *changes* in activity between conditions and therefore cannot directly assess the regional cerebral blood flow (rCBF) associated with a single state (for example, rCBF at rest or rCBF in a drug state). Because of the limitations of BOLD fMRI, we have previously used $H_2{}^{15}O$ based positron emission tomography to study the effect of propofol, a commonly used anesthetic drug, on brain areas functionally associated with wakefulness and the processing of pain. [3] This diffusible tracer based perfusion technique requires repeated arterial blood sampling, the availability of a cyclotron to produce the radiotracer and the number of scans are limited by the safe maximum dose of the radiotracer, $H_2{}^{15}O$.

Noninvasive alternatives to positron emission tomography are arterial spin labeling (ASL) MRI methods. ASL is accomplished by inverting spins upstream of the imaging slice at which perfusion is to be measured,[4, 5] so that the inverted magnetization of the blood water acts as a tracer. With pulsed arterial spin labeling techniques, a volume of blood is labeled upstream of the region of interest by a short radiofrequency pulse. With continuous arterial spin labeling techniques (CASL), an inversion pulse is applied continuously in the direction of flow. In addition to quantifying rCBF increases, this method allows us to examine whether certain pain tasks induce a *reduction* in rCBF, a possibility that is being overlooked by many BOLD fMRI based studies.[6] However, some early positron emission tomography reports indicated that task related blood flow reductions do occur in certain pain states [7–9]

We tested the hypothesis that cold, heat and ischemic pain induce the different rCBF changes within regions considered part of the "pain matrix"[10] using CASL fMRI. Instead of using very brief pain pulses characteristic for BOLD fMRI studies, we utilized sustained stimuli that would be perceived as moderately to severely painful without incurring the risk of tissue damage (cold and ischemic pain). Sustained tasks such as ischemic pain and the cold pain are thought to represent clinical pain better due to their psychophysical qualities [11–13] and are predictive of clinically relevant doses of analgesics [14–16] as well as acute and chronic pain-related clinical outcomes.[17, 18] We expected the side-by-side comparison of the pain tasks to reveal characteristic differences in brain activation. Finally, we examined some potential relationships between rCBF and individual pain tolerance levels.

Capturing data to evaluate pain type specific brain activation would help us to examine the utility of pain imaging as a marker for analgesic treatments. Information on the correlation of pain tolerance and cerebral blood flow would indicate whether subjective experience of pain reflects an individual's task induced cerebral blood flow.

## MATERIALS AND METHODS

### Subjects

The Institutional Review Board of the University of Alabama at Birmingham approved this study. Recruitment was performed by public advertisement around the university campus. Interested individuals were scheduled for a screening visit during which we determined eligibility by obtaining a medical history. We performed a focused physical examination and obtained written informed consent. Enrollment started in April 2009 and finished on January 2012. Inclusion criteria were right-handed healthy adults, age 19 to 50 yr, who were able to understand all study instructions. Handedness was assessed using the Edinburgh Handedness Inventory.[19] Exclusion criteria were any existing and active medical conditions that could affect somatosensation or cognitive function such as diabetes mellitus, neurologic diseases,

chronic pain, psychiatric disorders, the treatment with any scheduled medication and a past history of drug or substance abuse. Volunteers were paid for their participation and scheduled for a visit to obtain psychophysical measures and functional imaging on separate days.

Pain thresholds were obtained for each participant using a small 3-by-3 inch thermal probe (Thermal Sensory Analyzer TSA-II, Medoc Ltd., Ramat Yishai, Israel) applied to the skin of the forearm. Detection of the pain tolerance were assessed on the ventral forearm using an ascending method of limits with a 1 °C/s rate of rise (heat) whereby participants felt the temperature rise of the heat probe and were instructed to terminate the task by clicking a mouse button whenever they were no longer able to tolerate the thermal stimulus.

## Experimental Pain Tasks

Subjects underwent CASL imaging at rest and while experiencing three pain conditions. The order of study acquisitions for all participants was: Survey scan (1 min) for slice orientation, CASL rest (no pain stimulus), CASL heat, CASL ischemic, CASL cold pain and anatomical (T1-weighted) image. The rest scan was approximately 8 min for the acquisition of 42 tagged and untagged images, each pain session was approximately 5.5 min long for the acquisition of 30 tagged and untagged images and anatomical scans were approximately 1 (survey scan) and 6 min in duration. There was an approximately 5-min wait period between imaging sessions to advance the scanner settings and to adapt the stimulation set up. Participants remained in the scanner during setup and these steps for a total time of approximately 60 min.

To induce sustained but tolerable cold pain, we alternated the immersion of the volunteer's right hand into plastic cups filled with either ice water (2–3 °C) or tepid water (30 °C) for 10 s at a time during the cold pain imaging session. Heat pain was delivered using an MRI compatible, size 3-by-3 inch thermal probe (Medoc Ltd.) which was firmly applied to the right forearm of the participant. Each heat block consisted of an 8-s thermal stimulus that was programmed to fluctuate in a sinusoidal pattern within 46 to 49.5 degrees Celsius. Heat alternated with an 8-s block of neutral (32 degree Celsius) temperature. The reason for alternating blocks of pain with a neutral stimulus in the cold and heat pain conditions was to avoid habituation. If we had applied a constant thermal (cold or heat) stimulus, the intensity would have had to be relatively low to make it tolerable for participants.

Unlike the thermal tasks, the ischemic task was maintained continuously for the 5-min duration of the scan session. This standardized task had the participant elevate the right arm for 30 s, after which a cuff covering the upper arm was inflated to 250 mm Hg. The participant was then instructed to perform handgrip exercises for 1 min. Upon completion of the handgrip exercises, the imaging session was started.

## Imaging Parameters and Preprocessing

High-resolution structural MRI and quantitative ASL perfusion MRI were obtained at the University of Alabama cardiovascular imaging facility using a 3T MR Phillips Achieva scanner (Phillips Healthcare, Andover, MA). Structural imaging was performed with a T1-weighted 3D MPRAGE sequence with TR/TI/TE = 1,620/950/3msec, flip angle = 30°, matrix = 192×256×160, and voxel size = 0.98×0.98×1mm$^3$. ASL images were acquired using a CASL sequence with the following parameters: 1,600 Hanning window shaped pulses for a total labeling time = 2.4 s, post-labeling delay = 1.4 s, FOV = 230 mm, matrix = 128×128, bandwidth = 3kHz/pixel, TR/TE = 5000/56 ms, 13 slices with thickness of 7 mm plus 1.25 mm gap, mean Gz of 0.6mT/m, labeling was placed at 80 mm below the center of imaging region. 42 tag/control image pairs were acquired during the resting state, and 30

tag/control image pairs were acquired at each pain stimulation condition. Respiratory rate (RR) and end-tidal carbon dioxide values were recorded during each scan by sampling from a nasal cannula connected to a Capnomac Ultima carbon dioxide and anesthesia analyzer (General Electrics Healthcare, Waukesha, WI).

ASLtbx[20], an ASL data processing toolbox based on Matlab (Mathworks, Natick, MA) and SPM (Wellcome Department of Cognitive Neurology, London, United Kingdom) were used for imaging analysis. The following preprocessing steps were used: motion correction, residual motion effect removing, denoising, registration, spatial smoothing, CBF calculation, and CBF map spatial normalization. Both the labeled and control images were realigned together using the six parameters-based rigid body transformation to minimize the distance between each image and the reference volume. The algorithm was implemented in SPM. Then, the zigzagged labeled/control spin labeling paradigm was used as regressor in the estimated motion time courses, and the cleaned motion time courses were finally used for real motion corrections. No low-pass filtering was applied for ASL data. Spatial-temporal noise reduction was then performed using principal component analysis.[21] The nonzero eigenvalue associated eigenvectors and their time-courses were extracted by applying principal component analysis along the spatial dimension of ASL data to avoid the computational problem of applying principal component analysis along the temporal dimension. Each image was projected into these eigenvectors to obtain the corresponding representation coefficients. The following criteria were used to discard the noise-related eigenvectors and the corresponding representing coefficients in order to further denoise the raw ASL data: 1) any eigenvectors whose time-courses were correlated with the zig-zagged label-control paradigm were reserved; 2) minor components of the remaining eigenvectors were discarded if they accounted for less than 1% of the total variance of the data before principal component analysis denoising.

## Calculation of Regional Cerebral Blood Flow

The motion corrected ASL scans were then compartmentalized into groups of control or labeled images. Signal changes between the control and labeled images are much lower compared to signal changes observed in BOLD imaging. It is thus imperative to obtain rCBF maps prior to transforming the images to Montreal Neurology Institute template. The variation of signal intensities within control and labeled set of images made it necessary to average signal values for all images within each compartment before we calculated the CBF values. Quantitative CBF maps were then calculated from the control-tag perfusion signal difference using a modified two-compartment ASL perfusion model [22]

$$f=\frac{\Delta M\cdot\lambda\cdot R_{1\alpha}\cdot\exp(\omega\cdot R_{1\alpha})}{2\cdot M_0\alpha}[1-\exp(-t\cdot R_{1\alpha})]^{-1} \quad \text{(Equation 1)}$$

where $f$ is CBF, $\Delta M$ is the difference signal between the control and label acquisitions, $R_{1\alpha}$ is the longitudinal relaxation rate of blood, $\tau$ is the labeling time, $\omega$ is the post labeling delay time, $\alpha$ is the labeling efficiency, $\lambda$ is blood/tissue water partition coefficient, and $M_0$ is approximated by the control image intensity. The parameters used in this study were $R_{1a}$ = 1/1,664 s, $\alpha$ = 0.85 $\lambda$ = 0.9 g/ml, $\tau$ = 2.4, s $\omega$. 1.4 s. The CBF maps so generated were then normalized to the Montreal Neurology Institute template and smoothed using a 8 mm × 8 mm × 8 mm Gaussian kernel.

## Selection of Regions of Interest (ROIs)

Based on the existing literature on pain imaging we selected the following ROIs: thalamus, pre- and postcentral cortex, insular cortex, cingulate gyrus, anterior and posterior cingulum, amygdala, hippocampus, and Brodmann areas 1 to 4 and 6.[23] These ROIs were selected with

the Wake Forest University (Winston-Salem, North Carolina) pick atlas which uses the Talairach Daemon database.[24] From within these ROIs, we extracted the voxel signal intensities of labeled and unlabeled images and calculated rCBF as described in equation 1.

## Statistical Analysis Steps

We used the statistical software SAS (SAS Institute, Cary, NC) version 9.2, procedures GLM, MIXED, TTEST, and UNIVATIATE, for our statistical analysis.

**Analysis 1. Preliminary Analyses—**As preliminary, diagnostic analysis steps we compared global cerebral blood flow (blood flow of all voxels within the brain), RR and end-tidal carbon-dioxide to assure that these variables did not change significantly when comparing conditions (baseline and pain conditions) in separate analyses. The model for the global blood flow analysis was the following general linear model:

$$\mathrm{CBF}=\alpha+\beta_1*\mathrm{ID}+\beta_2*\mathrm{PC}+\varepsilon, \quad \text{(model 1)}$$

where *CBF* represents global cerebral blood flow, α represents the intercept, $\boldsymbol{\beta_1}$ represents the parameter vector associated with the subject effect (***ID***) and $\boldsymbol{\beta_2}$ represents the parameter vector associated with the three pain conditions. In this analysis, we did not consider subject as random effects since we were interested in obtaining a parameter estimate for the subject effect to inform us about the differences of global blood flow across participants.

While the latter analyses used blood flow data from all voxels within the brain, subsequent analyses were restricted to voxels within the regions of interest. RR and end-tidal carbon-dioxide were compared to resting baseline levels for each across pain conditions using paired *t*-tests. We considered a Bonferroni adjustment of the probability for rejecting the statistical null hypothesis ($\alpha = 0.05/3$) for the latter analysis.

**Analysis 2. Comparison of Pain Conditions—**We then directed our attention to our ROIs, grey matter regions functionally associated with pain. To better select voxels associated with grey matter we adopted the approach of selecting voxels with higher rCBF values. The method of selecting voxels with higher flow values has been used routinely in the analysis of SPECT data and is one of several approaches to avoid the inclusion of voxels that contain a mixture of multiple tissue values, also known as partial volume effect. [25, 26] We chose the top 50% selection criteria for subsequent statistical analyses. We compared cerebral blood flow change (baseline *vs.* pain) for each of the three pain conditions. In this comparison we controlled for the subject specific (cerebral blood flow) effects by entering subjects as random variable. We used the following mixed model:

$$\Delta\mathrm{rCBF}=\alpha+id+\beta*\mathrm{PC}+\varepsilon, \quad \text{model 2}$$

where *id* represents the subject random effect and ***PC*** represents pain condition vector, the explanatory variable of interest. Epsilon (ε) represents the residual error. We planned to compare pain conditions with *t*-tests as follow up procedure if the overall model showed significant differences.

**Analysis 3. Blood Flow Changes across ROIs—**To quantify rCBF changes across ROIs, we used a mixed model where subjects were entered as random variable, pain condition was nested within the subject effect and regions of interest were entered as fixed effect:

$$\Delta\mathrm{rCBF}=\alpha+id[\mathrm{PC}]+\beta_1*\mathrm{PC(ROI)}+\beta_2*\mathrm{ROI}+\varepsilon, \quad \text{(model 3)}$$

where *id*[***PC***] represents the subject random variable nested within pain conditions (***PC***) with associated parameter vector $\beta_1$, ***PC***(***ROI***) represents the pain condition nested within ***ROI*** with associated parameter vector $\beta_2$ and epsilon ($\varepsilon$) represents the residual error.

**Analysis 4. Correlation of Pain Tolerance and Cerebral Blood Flow—**We then determined whether participant's pain tolerance was correlated with CBF using a bivariate regression with heat pain tolerance as explanatory variable and mean rCBF, averaged across ROIs, as outcome variable:

$$\mathrm{rCBF}=\alpha+\beta*\mathrm{HPTo}+\varepsilon \quad \text{(model 4)}$$

where $\alpha$ represents the intercept, $\beta$ represents the parameter vector for each participants' heat pain tolerance (***HPTo***) and $\varepsilon$ represented the residual error. We performed separate analyses for each of the three pain conditions and considered a Bonferroni adjustment of the probability for rejecting the statistical null hypothesis ($\alpha = 0.05/3$). *Heat* pain tolerance was used as tolerance measure because it is a widely published and reliable method.

**Analysis 5. SPM Analysis without Restriction to ROIs—**Finally, we determine whether a similar pattern of brain activity would be observed if the analysis was carried out without restriction to regions of interest. After data preprocessing as described above, this analysis was carried out using the general linear model [27] built into statistical parametric mapping (SPM version 8). A general linear mixed model was used to generate a statistical probability map for the group analysis. [28] The latter is referred to in SPM as second level analysis.

## RESULTS

Participants consisted of five men and five women. The median age was 31 yr with a range from 19 to 49 yr. Six participants were African American and four participants were White.

### Results of Analysis 1 (Global Cerebral Blood Flow)

We observed that global cerebral blood flow differed across participants ($F = 73.40$, $p < 0.001$). When accounting for those subject specific global cerebral blood flow, global CBF values did not differ statistically ($p = 0.2406$) across conditions. We illustrate the effect of selecting the top 20% and 50% flow values in figure 1. This figure is also suitable to contrast and compare rCBF and the shape of rCBF distributions.

Average participants' RR at rest was 15.6 ± 3.8 and the end-tidal carbon-dioxide level at rest was 38.6 ± 2.4. During the cold condition average participants' RR was 16.3 ± 3.2 and end-tidal carbon-dioxide level was 38.5 ± 3.3. During the heat condition average patients' RR was 15.9 ±3.5 and end-tidal carbon-dioxide level was 39.0 ± 3.2. During the ischemic condition RR was RR=16.1 ± 4.0 and end-tidal carbon dioxide level was 39.1 ± 3.3. Respiratory rate and end-tidal carbon-dioxide levels during each pain condition were not statistically different from their resting baseline values: $p = 0.9391$ (t-ratio = 0.0775) for rest *versus* cold, $p = 0.755$ (t-ratio= 0.3162) for rest *versus* heat and $p = 0.7029$ (t-ratio = 0.3875) for rest *versus* ischemia.

### Results of Analysis 2 (Comparison of Pain Conditions)

Figure 1 shows the distribution of rCBF values within our ROIs as boxplots and histograms by condition. It can be seen that blood flow values at rest cover a relatively large range of values. During the cold pain condition, blood flow values tend to have a more unimodal (centered) distribution. Compared to the resting condition, a change in the shape of the

histogram can also be seen for heat and ischemic pain. When comparing rCBF values across ROIs in the mixed model analysis, we observed a significant difference in rCBF change (Pain *vs.* Rest, $p < 0.0001$). Regional CBF within the pain matrix (averaged across pain ROIs) showed a small increase for the cold pain task [rCBF Change (ΔrCBF) = 0.35 ml/100g/min] and heat pain [ΔrCBF = 1.00 ml/100g/min] but ischemic pain showed a significant rCBF reduction [ΔrCBF = −3.70 ml/100g/min].

### Analysis 3: Blood Flow Changes across ROIs

We found a significant difference in rCBF change (ΔrCBF) when comparing ROIs. These are listed in table 1 and changes are illustrated in figure 2. By designating "subject" nested within "pain condition" as random effect in this mixed model we accounted for the randomness of rCBF due participants' biological differences. The overall model fit was very good (adjusted $R^2 = 0.893$, $p < 0.0001$). We observed that the pain condition effect, nested within ROI was not significant (F-ratio = 0.960, $p = 0.561$) but the ROI effect was (F-ratio = 1.740, $p = 0.0105$). This indicated that observed change in regional cerebral blood flow (ΔrCBF) depended on the anatomical location within the pain matrix, which we refer to as ROI. To determine which of the anatomical brain regions of interest showed the most change, we evaluated the parameter estimates for each region of interest and observed a 2.491 ml/100g/min rCBF decreases in both cerebellar hemispheres (t-ratio = −3.09, $p = 0.0024$), a 2.291 ml/100g/min rCBF increase to the anterior cingulate gyrus (t-ratio = 3.28, $p = 0.0011$), a 1.853 ml/100g/min increase rCBF increase to the left amygdala (t-ratio = 2.93, $p = 0.0035$), and a 1.670 ml/(100mg*min) rCBF increase in BA 6 (t-ratio = 2.238, $p = 0.0238$).

Figure 3 shows CASL rCBF images of a case example as well as mean group rCBF images for the resting state and cold pain scans. It illustrates how rCBF increases in the ACC is evident in the single case and are also confirmed in general in the group data. The coordinates and planes shown also capture some of the marked activity increase in BA 6.

### Analysis 4: Association of Pain Tolerance and rCBF

We observed a significantly higher rCBF in response to cold pain in individuals with higher pain tolerance ($p = 0.0314$). Given the Bonferroni adjustment, this difference is not statistically significant but can be described as an important trend. No association was observed for either heat or ischemic pain.

### Analysis 5: SPM of CASL Images

The results of statistical parametric mapping analyses by pain task are listed in tables 2–4 and illustrated in figure 4. These results differ somewhat from the direct analysis because in the SPM analysis we did not restrict our search to pain ROIs. We list areas of the brain that meet the uncorrected statistical threshold of $p = 0.001$. The observed changes agree with our ROI based analysis in several key areas. With respect to the cold task, the most notable finding is the activation of brain areas functionally associated with somatosensory processing (pre- and postcentral gyrus) and integration (BA 6). We found heat pain to be associated with activation in the anterior cingulate gyrus bilaterally, left insula (Rolandic operculum) and inferio-parietal cortex. We found ischemic pain to be associated with an rCBF increase in the left insula and thalamus whereas BA 6 and postcentral gyrus show deactivation (reduced rCBF) with this modality.

## DISCUSSION

The most salient findings of our study - in detail described in the following subheadings - are that (a) pain – related rCBF changes are task specific and (b) across modalities the most

consistent change can be observed in the supplemental motor cortex (BA 6) rather than brain regions associated with somatosensory brain areas. We introduce CASL imaging as a method to quantify state dependent pain measures. This is clinically relevant since, in the practice of anesthesiology, we are concerned with drug states such as the state of anxiety (prior to surgery), the sedated state (during a clinical procedure) or the analgesic state (of a patient having received opioid analgesics). As objective measures of changes in central nervous system activity that can be task and state specific, CASL imaging allows for the assessment of complex cognitive processes and how these activities can be altered by manipulations such as anesthesia.

## Detecting Pain Task specific rCBF Patterns

One of the most striking observations was the *reduction in rCBF within the pain ROIs seen with ischemic pain*, whereas thermal (cold and heat) pain showed no net change or a net increase in rCBF. Upon closer examination, we can appreciate that the overall pattern of the blood flow distribution is similar to the one observed in other pain modalities (fig. 2). As described, we estimated "global cerebral blood flow" by calculating the mean of all brain voxels with a nonzero rCBF. We observed a small reduction of global CBF in the cold condition when compared to the resting state whereas no change of global blood flow was observed for the ischemic condition. By contrast, within the pain ROIs, cold pain resulted in a net blood flow increases and ischemic pain resulted in a net blood flow decrease. While most of the BOLD fMRI literature focuses on areas with relative signal increases, task related blood flow reductions have been reported before.[7–9] These small changes in global rCBF during the cold and ischemic task may represent minimal effects of peripheral circulation changes not completely adjusted for by global cerebral autoregulation.[29] This finding calls attention to the need for close examination of relative signal or rCBF decreases when examining and describing the effects of pain.

## Brodmann Area 6 as Potential Biomarker of Acute Pain

We found BA6 to receive significantly higher rCBF across pain modalities. This relatively large cortical area represents a bilaterally organized system involved in the acquisition and performance of skilled motor acts including speech and writing [30] and preparation for and the sensory guidance of movement [31–33].

An intuitive explanation for the activation of BA6 activated across pain modalities is based on its involvement in the planning of motor responses. In our experiment participants did not move the right arm, despite its subjection to the pain task, presumably suppressing the urge to withdraw the arm from the painful stimulus. The supplemental motor area (BA6) and ventrolateral prefrontal cortex have been implicated in the suppression of a motor task [34]. This is consistent with a recently documented cognitive role of BA6; Tanaka *et al* [35] reported BA6 activation in response to both verbal and spatial mental operation using BOLD fMRI and a decreased performance of the mental operation if subjects received transcranial stimulation to BA6. Within this context, the blood flow change we observed may be best described as an associated cognitive mental response. Though activation of the supplemental motor area has been observed in other studies, we highlight this area in our discussion since it was both significant across pain tasks and draws attention to the potential utility of monitoring the motor response to a painful stimulus as a means of assessing the efficacy of an analgesic intervention which does not rely on a patient's subjective interpretation of a painful stimulus. This finding is clinically relevant since one of the main goals of pain imaging is to find an objective measure of analgesia.

### Subjective Pain Tolerance and rCBF

The notable correlation observed between individual pain tolerance measures, which reflect a person's subjective experience, and rCBF during the cold condition, without doubt an objective measure, is a very promising relationship suggesting the possibility of using certain rCBF measures as a biomarker of pain. It is interesting to note that there is some evidence to suggest that pain, when persistent, is associated with characteristic changes in rCBF. [36–38] Although the correlation observed in these studies may not be robust enough to suggest making clinical decisions about individual cases, these data suggest that the promise of imaging biomarkers of certain perceptual states may be realizable. Issues such as drug seeking behavior, potential secondary gain, and underlying psychological and social stressors often confound a patient's self-report of pain. Health care providers are therefore keenly interested in a more objective method of assessing pain. Imaging methods that can quantitatively measure metabolic activity associated with particular states, such as CASL, probably offer the best hope for imaging biomarkers of acute and possibly also chronic painful conditions.

### Comparison of Region of Interest based *versus* Global (SPM) Analysis

SPM analysis revealed a number of regional findings similar to the findings in the ROI based analysis, but they appear more sporadic in terms of which pain condition elucidates them. As noted above, SPM analysis showed "deactivation" in several regions (BA 6 and postcentral gyrus) during the ischemic task that was consistent with the absolute rCBF reduction seen on ROI analysis. SPM also showed "activation" in the thalamus and insula in the ischemic condition, regions showing less rCBF reduction (than the mean) in the ROI analysis. Though clearly not identical in terms of statistical significance across all findings, our direct ROI analysis and the SPM analysis of normalized whole brain data show a great deal of overlap. We presume that differences are due to a combination of factors, including SPM's adjustment for global changes and to the more conservative thresholds that need to be used when evaluating the entire brain, combined with the lower signal associated with the CASL (as opposed to BOLD fMRI) method. Surprisingly, SPM analysis of the whole brain did not reveal additional findings to the ROI analysis, attesting in part to the relative theoretical completeness of the ROIs examined, the relatively conservative thresholds applied to whole brain data, and perhaps the lower signal strength of ASL masking weaker activation effects.

The CASL imaging method used here appears to have great potential for the comparison of within subject changes associated with state changes or interventions and between subject baseline differences in rCBF. Future studies using this technique in targeted clinical pain populations are likely to reveal patterns of cerebral blood flow that prove to have clinical utility on both the group and individual case level.

## Acknowledgments

The authors would like to acknowledge the assistance of Alice Esame B.S. (Research Assistant, Department of Anesthesiology, University of Alabama at Birmingham), and Catiffaney Banks, B.S. (Research Assistant, Department of Anesthesiology) for their research coordination efforts and the advice of Ze Wang, Ph.D. (Assistant Professor of Biomedical Engineering, Department of Psychiatry, School of Medicine, Dept. of Bioengineering, School of Engineering and Applied Science, University of Pennsylvania, Philadelphia, Pennsylvania) and Jan d, en Hollander, Ph.D. (Professor, Department of Medicine, University of Alabama at Birmingham) for this project.

Support: National Institute of Health, Bethesda, Maryland, K23RR021874, American Society of Regional Anesthesia and Pain Medicine, Schaumburg, Illinois, Carl Koller Grant 2010, and the University of Alabama Radiology Research Initiative Pilot Award.

## REFERENCES


1. Tracey I. Imaging pain. Br J Anaesth. 2008; 101:32–39. [PubMed: 18556697]
2. Bingel U, Tracey I. Imaging CNS modulation of pain in humans. Physiology (Bethesda). 2008; 23:371–380. [PubMed: 19074744]
3. Byas-Smith M, Frolich MA, Votaw JR, Faber TL, Hoffman JM. Cerebral blood flow during propofol induced sedation. Mol Imaging Biol. 2002; 4:139–146. [PubMed: 14537136]
4. Barbier EL, Lamalle L, Decorps M. Methodology of brain perfusion imaging. J Magn Reson Imaging. 2001; 13:496–520. [PubMed: 11276094]
5. Detre JA, Leigh JS, Williams DS, Koretsky AP. Perfusion imaging. Magn Reson Med. 1992; 23:37–45. [PubMed: 1734182]
6. Peyron R, Laurent B, Garcia-Larrea L. Functional imaging of brain responses to pain: A review and meta-analysis. Neurophysiol Clin. 2000; 30:263–288. [PubMed: 11126640]
7. Allison JD, Meador KJ, Loring DW, Figueroa RE, Wright JC. Functional MRI cerebral activation and deactivation during finger movement. Neurology. 2000; 54:135–142. [PubMed: 10636139]
8. Shmuel A, Augath M, Oeltermann A, Logothetis NK. Negative functional MRI response correlates with decreases in neuronal activity in monkey visual area v1. Nat Neurosci. 2006; 9:569–577. [PubMed: 16547508]
9. Smith AT, Singh KD, Greenlee MW. Attentional suppression of activity in the human visual cortex. Neuroreport. 2000; 11:271–277. [PubMed: 10674469]
10. Legrain V, Iannetti GD, Plaghki L, Mouraux A. The pain matrix reloaded: A salience detection system for the body. Prog Neurobiol. 2011; 93:111–124. [PubMed: 21040755]
11. Bhalang K, Sigurdsson A, Slade GD, Maixner W. Associations among four modalities of experimental pain in women. J Pain. 2005; 6:604–611. [PubMed: 16139779]
12. Frolich MA, Bolding MS, Cutter GR, Ness TJ, Zhang K. Temporal characteristics of cold pain perception. Neurosci Lett. 2010; 480:12–15. [PubMed: 20493237]
13. Rainville P, Feine JS, Bushnell MC, Duncan GH. A psychophysical comparison of sensory and affective responses to four modalities of experimental pain. Somatosens Mot Res. 1992; 9:265–277. [PubMed: 1492527]
14. Enggaard TP, Poulsen L, Arendt-Nielsen L, Hansen SH, Bjornsdottir I, Gram LF, Sindrup SH. The analgesic effect of codeine as compared to imipramine in different human experimental pain models. Pain. 2001; 92:277–282. [PubMed: 11323149]
15. Moore PA, Duncan GH, Scott DS, Gregg JM, Ghia JN. The submaximal effort tourniquet test: Its use in evaluating experimental and chronic pain. Pain. 1979; 6:375–382. [PubMed: 460938]
16. Posner J. A modified submaximal effort tourniquet test for evaluation of analgesics in healthy volunteers. Pain. 1984; 19:143–151. [PubMed: 6462726]
17. Edwards RR, Doleys DM, Lowery D, Fillingim RB. Pain tolerance as a predictor of outcome following multidisciplinary treatment for chronic pain: Differential effects as a function of sex. Pain. 2003; 106:419–426. [PubMed: 14659525]
18. Soyupek S, Bozlu M, Armagan A, Ozorak A, Perk H. Does experimental pain assessment before biopsy predict for pain during transrectal ultrasound-guided prostate biopsy? Urology. 2007; 70:681–684. [PubMed: 17991537]
19. Oldfield RC. The assessment and analysis of handedness: The edinburgh inventory. Neuropsychologia. 1971; 9:97–113. [PubMed: 5146491]
20. Wang Z, Aguirre GK, Rao H, Wang J, Fernandez-Seara MA, Childress AR, Detre JA. Empirical optimization of ASL data analysis using an ASL data processing toolbox: ASLtbx. Magn Reson Imaging. 2008; 26:261–269. [PubMed: 17826940]
21. Thomas CG, Harshman RA, Menon RS. Noise reduction in bold-based fMRI using component analysis. Neuroimage. 2002; 17:1521–1537. [PubMed: 12414291]
22. Parkes LM. Quantification of cerebral perfusion using arterial spin labeling. Two-compartment models. J Magn Reson Imaging. 2005; 22:732–736. [PubMed: 16267854]
23. Tracey I, Johns E. The pain matrix: Reloaded or reborn as we image tonic pain using arterial spin labelling. Pain. 2010; 148:359–360. [PubMed: 20080346]

24. Lancaster JL, Woldorff MG, Parsons LM, Liotti M, Freitas CS, Rainey L, Kochunov PV, Nickerson D, Mikiten SA, Fox PT. Automated talairach atlas labels for functional brain mapping. Hum Brain Mapp. 2000; 10:120–131. [PubMed: 10912591]
25. Deutsch G, Mountz JM, Katholi CR, Liu HG, Harrell LE. Regional stability of cerebral blood flow measured by repeated technetium-99m-HMPAO SPECT: Implications for the study of state-dependent change. J Nucl Med. 1997; 38:6–13. [PubMed: 8998141]
26. Iida H, Law I, Pakkenberg B, Krarup-Hansen A, Eberl S, Holm S, Hansen AK, Gundersen HJ, Thomsen C, Svarer C, Ring P, Friberg L, Paulson OB. Quantitation of regional cerebral blood flow corrected for partial volume effect using o-15 water and pet: I. Theory, error analysis, and stereologic comparison. J Cereb Blood Flow Metab. 2000; 20:1237–1251. [PubMed: 10950386]
27. Penny W, Friston K. Mixtures of general linear models for functional neuroimaging. IEEE Trans Med Imaging. 2003; 22:504–514. [PubMed: 12774896]
28. Friston KJ, Stephan KE, Lund TE, Morcom A, Kiebel S. Mixed-effects and fMRI studies. Neuroimage. 2005; 24:244–252. [PubMed: 15588616]
29. Aries MJ, Elting JW, De Keyser J, Kremer BP, Vroomen PC. Cerebral autoregulation in stroke: A review of transcranial doppler studies. Stroke. 2010; 41:2697–2704. [PubMed: 20930158]
30. Freund HJ. Premotor area and preparation of movement. Rev Neurol (Paris). 1990; 146:543–547. [PubMed: 2263816]
31. Wise SP. The primate premotor cortex: Past, present, and preparatory. Annu Rev Neurosci. 1985; 8:1–19. [PubMed: 3920943]
32. Picard N, Strick PL. Motor areas of the medial wall. A review of their location and functional activation. 1996; 6:342–353.
33. Tanji J. New concepts of the supplementary motor area. Curr Opin Neurobiol. 1996; 6:782–787. [PubMed: 9000016]
34. Tabu H, Mima T, Aso T, Takahashi R, Fukuyama H. Common inhibitory prefrontal activation during inhibition of hand and foot responses. Neuroimage. 2011; 59:3373–3378. [PubMed: 22079449]
35. Tanaka S, Honda M, Sadato N. Modality-specific cognitive function of medial and lateral human brodmann area 6. J Neurosci. 2005; 25:496–501. [PubMed: 15647494]
36. Apkarian, AV. Human brain imaging studies of chronic pain: Translational pain research: From mouse to man. Boca Raton, FL: CRC Press; 2010.
37. Ness TJ, San Pedro EC, Richards JS, Kezar L, Liu HG, Mountz JM. A case of spinal cord injury-related pain with baseline rCBF brain SPECT imaging and beneficial response to gabapentin. Pain. 1998; 78:139–143. [PubMed: 9839825]
38. Coghill RC, McHaffie JG, Yen YF. Neural correlates of interindividual differences in the subjective experience of pain. Proc Natl Acad Sci U S A. 2003; 100:8538–8542. [PubMed: 12824463]
39. Caspers S, Geyer S, Schleicher A, Mohlberg H, Amunts K, Zilles K. The human inferior parietal cortex: Cytoarchitectonic parcellation and interindividual variability. Neuroimage. 2006; 33:430–448. [PubMed: 16949304]
40. Caspers S, Eickhoff SB, Geyer S, Scheperjans F, Mohlberg H, Zilles K, Amunts K. The human inferior parietal lobule in stereotaxic space. Brain Struct Funct. 2008; 212:481–495. [PubMed: 18651173]
41. Amunts K, Kedo O, Kindler M, Pieperhoff P, Mohlberg H, Shah NJ, Habel U, Schneider F, Zilles K. Cytoarchitectonic mapping of the human amygdala, hippocampal region and entorhinal cortex: Intersubject variability and probability maps. Anat Embryol (Berl). 2005; 210:343–3452. [PubMed: 16208455]

## Summary Statement

**What we know about this topic**

The pattern of cerebral activity associated with states such as a sustained pain state or changes due to a neurotropic drug are not well characterized

**What new information this study provides**

Using continuous arterial spin labeling, regional cerebral blood flow changes were characteristic of a pain task employed and may provide evidence for an imaging biomarker of pain

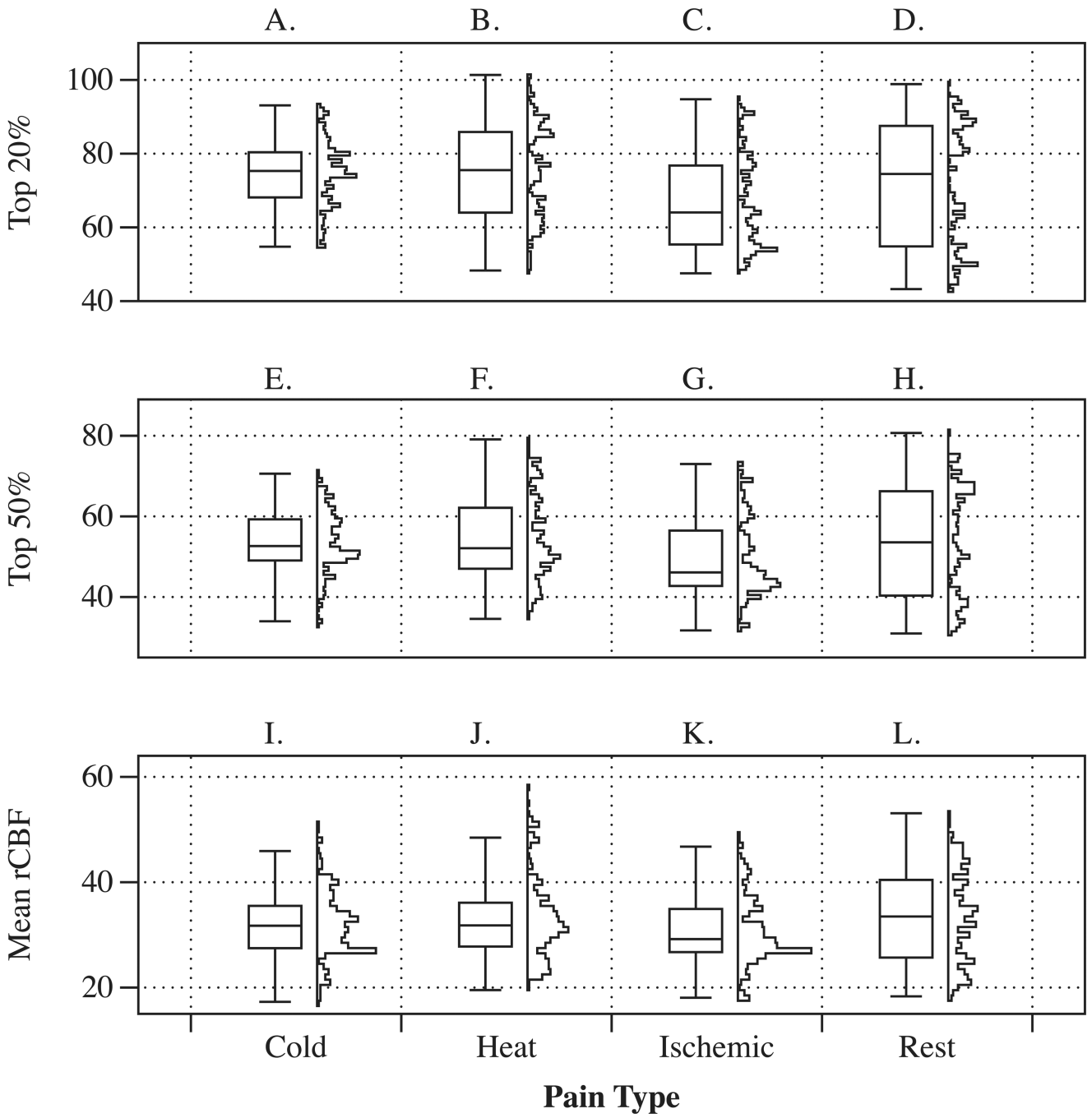


**Figure 1.**

The figure shows corresponding boxplots and vertical histograms of rCBF values calculated separately for each region of interest and each participant. Panels A to D illustrate summary plots for the top 20% blood flow data. Panels E to H illustrate summary plots for the top 50% blood flow data and Panels I to L illustrate summary plots for the top mean (average) blood flow data. The categorical axis (x-axis) shows experimental conditions. Regions of interest included were BA 1–4, BA 6 insular and cingulate cortex, amygdala, hippocampus, thalamus and cerebellum. rCBF: regional cereral blood flow; BA: Brodman area.

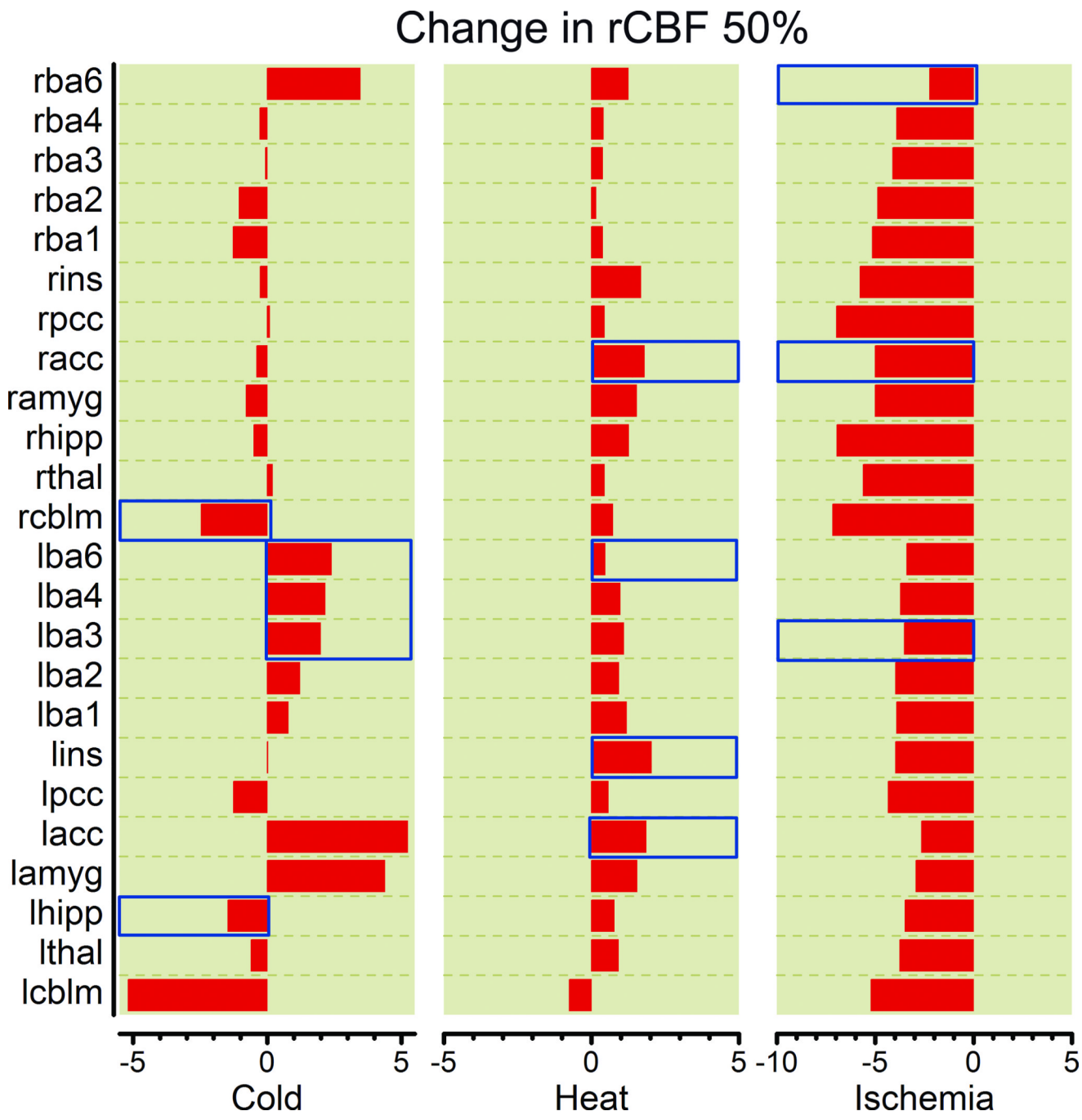


**Figure 2.**

Average regional cerebral blood flow values in ROIs using the top 50% voxel selection filter. Areas that can also be identified in the by the SMP analysis that was not restricted to pain ROIs are marked with a transparent red overlay bar. ROI: region of interest; rCBF: regional cerebral blood flow.

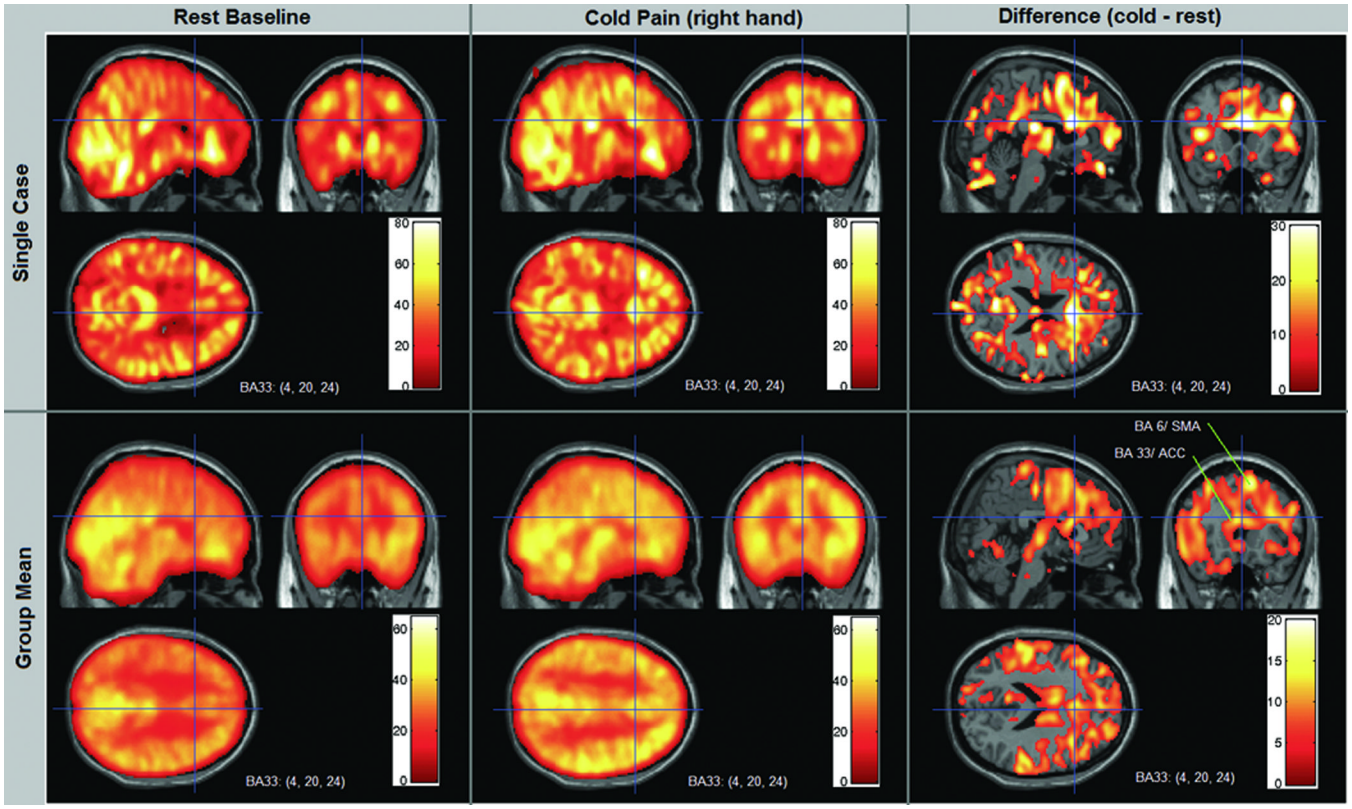


**Figure 3.**

CASL rCBF images for a single case and for the mean of all 10 cases during Rest and the Cold Pain condition. In this example the crosshairs and corresponding orthogonal slices are centered on the anterior cingulate cortex (ACC), Montreal Neurology Institute coordinates x= 4, y=20, z=24. The group images were created from the mean of 10 motion corrected individual case image sets, spatially normalized into stereotactic space. Color bar scales indicate rCBF in ml/100g/min. Increased rCBF is evident in the ACC during cold pain by visual inspection of the case example (the actual rCBF increases from 49.6 at rest to 72.9 at the coordinate center voxel). The group mean images show that this increase is evident across subjects, both by visual inspection and quantitative values (group mean rCBF increases from 41.9 to 57.4 at the coordinate center voxel). The difference images on the right side were created by subtracting the resting baseline rCBF values from the cold pain rCBF values in all voxels. The ACC (BA 33) appears as the area of greatest flow increase in these coordinate planes, along with part of the supplementary motor cortex (BA 6) in these planes shown. The lower right panel identifies these two regions in the mean group subtraction. CASL: continuous arterial spin labeling; rCBF: regional cerebral blood flow; BA: Brodman area.

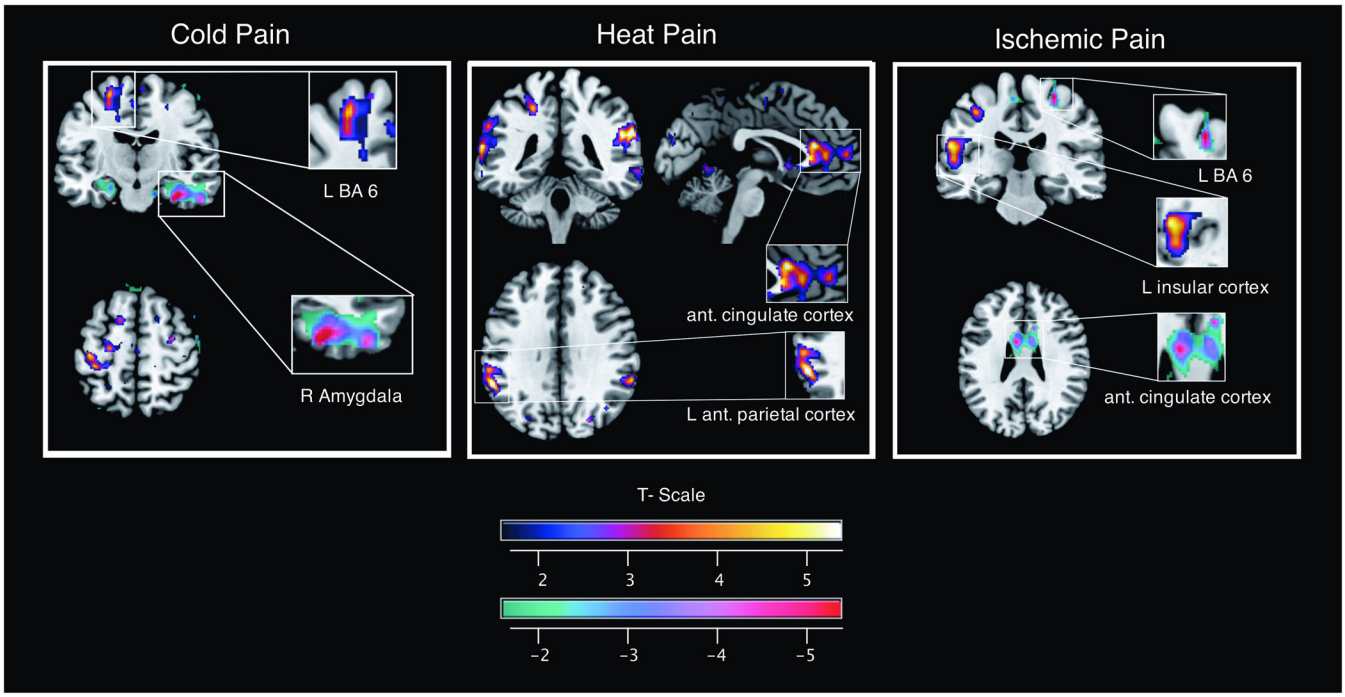


**Figure 4.**

Representative maps of increased and decreased rCBF for the cold pain, heat pain, and ischemic pain condition based on the SPM analysis. Relative signal change are coded using the NIH-fire color scheme (upper bar) for increase and the NIH-ice color scheme for rCBF reduction (lower bar). rCBF: regional cerebral blood flow; SPM: statistical parametric mapping; NIH: National Institute of Health; BA: Brodman area.

**Table 1**

rCBF Change in ROIs

| ROI | ΔrCBF | t-ratio | p-value (>\|t\|) | 95% CI Lower | 95% CI Upper |
|---|---|---|---|---|---|
| **lacc** | **2.291** | **2.8** | **0.005** | **0.684** | **3.897** |
| **lamyg** | **1.853** | **2.26** | **0.024** | **0.246** | **3.459** |
| lba1 | 0.366 | 0.45 | 0.655 | −1.241 | 1.972 |
| lba2 | 0.387 | 0.47 | 0.637 | −1.220 | 1.993 |
| lba3 | 0.785 | 0.96 | 0.338 | −0.822 | 2.391 |
| lba4 | 0.774 | 0.95 | 0.345 | −0.833 | 2.380 |
| lba6 | 0.688 | 0.84 | 0.400 | −0.918 | 2.295 |
| **lcblm** | **−2.491** | **−3.05** | **0.002** | **−4.098** | **−0.885** |
| lcing | 0.594 | 0.33 | 0.745 | −2.984 | 4.172 |
| lhipp | −0.312 | −0.38 | 0.703 | −1.919 | 1.294 |
| lins | 0.375 | 0.46 | 0.647 | −1.231 | 1.982 |
| lthal | −0.008 | −0.01 | 0.992 | −1.614 | 1.599 |
| racc | −0.189 | −0.23 | 0.817 | −1.796 | 1.417 |
| ramyg | −0.410 | −0.5 | 0.617 | −2.016 | 1.197 |
| rba1 | −0.872 | −1.07 | 0.287 | −2.478 | 0.735 |
| rba2 | −0.858 | −1.05 | 0.295 | −2.464 | 0.749 |
| rba3 | −0.241 | −0.3 | 0.768 | −1.848 | 1.365 |
| rba4 | −0.269 | −0.33 | 0.743 | −1.875 | 1.338 |
| **rba6** | **1.700** | **2.08** | **0.038** | **0.093** | **3.306** |
| **rcblm** | **−1.848** | **−2.26** | **0.024** | **−3.455** | **−0.242** |
| rcing | −0.682 | −0.83 | 0.405 | −2.289 | 0.924 |
| rhipp | −0.941 | −1.15 | 0.251 | −2.547 | 0.666 |
| rins | −0.241 | −0.29 | 0.769 | −1.847 | 1.366 |

lacc: left anterior cingulate cortex, lamyg:left amygdala, lba1–4,6: left Brodmann area 1–4,6. lcblm: left cerebellum, lcing; left cingulate gyrus, lhipp: left hippocampus, lins: left insula, lthal: left thalamus, racc: right anterior cingulate cortex, ramyg:right amygdala, rba1–4,6: right Brodmann area 1–4,6. rcblm: right cerebellum, rcing; right cingulate gyrus, rhipp: right hippocampus, rins: right insula, rthal: right thalamus.

**Table 2**

SPM Cold Pain

| | | | | | | |
|---|---|---|---|---|---|---|
| ***Activation*** | | | | | | |
| **X** | **Y** | **Z** | **Cluster Size** | **Anatomy I** | **Anatomy II** | **t-value** |
| −18 | 7 | 64 | 36 | L superior frontal gyrus | BA 6 | 7.07 |
| −20 | 55 | 32 | 28 | L superior frontal gyrus | | 8.82 |
| −48 | −74 | 20 | 17 | L middle temporal gyrus | IPC (PGp) | 4.81 |
| −40 | −22 | 57 | 15 | L precentral gyrus | BA 4a | 4.77 |
| | | | | | BA 6 | |
| −36 | −32 | 60 | 6 | L postcentral gyrus | BA 3b | 5.31 |
| | | | | | BA 4a | |
| −46 | 8 | 42 | 6 | L precentral gyrus | BA 44 | 5.09 |
| *Deactivation* | | | | | | |
| **X** | **Y** | **Z** | **Cluster Size** | **Anatomy I** | **Anatomy II** | **t-value** |
| 32 | −18 | −24 | | R para-hippocampal gyrus | Hipp (SUB) | 6.59 |
| | | | | | Hipp (CA) | |
| 36 | −16 | −26 | | R Fusiform Gyrus | Hipp (CA) | |
| 21 | 4 | −24 | 49 | R para-hippocampal gyrus | Hipp (EC) | 4.3 |
| 54 | −6 | −27 | 14 | R inferior temporal gyrus | | |

BA 6: Brodmann area 6, BA 4a: Brodmann area 4a, BA 3b: Brodmann area 3b, BA 4a: Brodmann area 4a, BA 44: Brodmann area 44, IPC (PGp): Inferior parietal cortex, area PGp[39,40], Hipp (SUB): Hippocampus area SUB, Hipp (CA)[41] Hippocampus area CA[41], Hipp (EC): Hippocampus area EC[41].

**Table 3**

SPM Heat Pain

***Activation***

| X | Y | Z | Cluster Size | Anatomy I | Anatomy II | t-value |
|---|---|---|---|---|---|---|
| 60 | −40 | 26 | 136 | R supramarginal gyrus | IPC (PF) | 6.79 |
| | | | | | IPC (PFm) | |
| 4 | 31 | 0 | 96 | R anterior cingulate cortex | (ACC) | 4.63 |
| 0 | 27 | 22 | | L anterior cingulate cortex | (ACC) | 5.46 |
| −54 | −68 | 4 | 87 | L middle temporal gyrus | | 6.35 |
| −57 | −47 | 30 | 79 | L supramarginal gyrus | IPC (PFm) | 6.53 |
| | | | | | IPC (PFcm) | |
| −32 | −17 | 62 | 15 | L precentral gyrus | BA 6 | 7.82 |
| 27 | 16 | −2 | 14 | R putamen | | 4.8 |
| −42 | −18 | 14 | 16 | L Rolandic operculum | OP 1 | 4.7 |
| | | | | | OP 4 | |

*Deactivation*

| X | Y | Z | Cluster Size | Anatomy I | Anatomy II | t-value |
|---|---|---|---|---|---|---|
| 51 | −6 | 56 | 3 | R middle frontal gyrus | | 4.9 |

IPC (PFm)[39,40] inferior Parietal Cortex area PFm, IPC (PFcm)[39,40] inferior Parietal Cortex area PFcm, BA 6: Brodmann area 6, OP 1: Parietal operculum area 1, OP 4: Parietal operculum area 4.

## Table 4

SPM Ischemic Pain

***Activation***

| X | Y | Z | Cluster Size | Anatomy I | Anatomy II | t-value |
|---|---|---|---|---|---|---|
| −57 | −29 | 18 | 95 | L superior temporal gyrus | OP 1 | 6.29 |
| | | | | | IPC (PFop) | |
| −36 | 9 | 10 | 88 | L insula lobe | | 9.66 |
| −45 | 32 | 9 | 18 | L inferior frontal gyrus | BA 45 | 4.99 |
| 16 | 64 | 0 | 18 | R superior orbital gyrus | | 6.75 |
| 5 | −55 | −67 | 14 | R middle temporal gyrus | hOC5 (V5) | 5.11 |
| 9 | −18 | 22 | 6 | R thalamus | | 4.65 |

*Deactivation*

| X | Y | Z | Cluster Size | Anatomy I | Anatomy II | t-value |
|---|---|---|---|---|---|---|
| 27 | −30 | 66 | 15 | R pre-central gyrus | BA 6 | > 4.3 |
| 34 | −4 | 65 | 8 | R middle frontal gyrus | BA 4p | 5.84 |
| 26 | 26 | −68 | 6 | R superior occipital gyrus | SPL (7p) | > 4.3 |
| 21 | −87 | −12 | 6 | R cerebellum | hOC3v | > 4.3 |
| 24 | −5 | −14 | 4 | R amygdala | Amy (SF) | > 4.3 |
| −52 | −27 | 64 | 2 | L post-central gyrus | | > 4.3 |
| 10 | 14 | 32 | 2 | R anterior cingulate cortex | | > 4.3 |

OP 1: parietal operculum area 1, IPC(PFop): inferior parietal lobe area PFop, BA 45: Brodmann area 45, hOC5 (V5): human occipital cortex area 5, BA 6: Brodmann area 6, BA 4p; Brodmann area 4p, SPL (7p): superior parietal lobe area 7p, hOC3y: human occipital lobe area 3y, Amy (SF): amygdala superficial.